Max H. Sherman[1] *and Mark P. Modera*[1]

Comparison of Measured and Predicted Infiltration Using the LBL Infiltration Model

REFERENCE: Sherman, M. H. and Modera, M. P., **"Comparison of Measured and Predicted Infiltration Using the LBL Infiltration Model,"** *Measured Air Leakage of Buildings, ASTM STP 904*, H. R. Trechsel and P. L. Lagus, Eds., American Society for Testing and Materials, Philadelphia, 1986, pp. 325–347.

ABSTRACT: The Lawrence Berkeley Laboratory (LBL) infiltration model was developed in 1980; since that time many simultaneous measurements of infiltration and weather have been made, allowing comparison of predictions with measured infiltration. This report presents the LBL model as it currently exists and summarizes infiltration measurements and corresponding predictions. These measurements include both long-term and short-term data taken in houses with climates ranging from the mild San Francisco Bay area to the more extreme Midwest. These data also provide a data base for comparison with other infiltration models and provide a starting point for the determination of the accuracy and precision of air infiltration models.

KEY WORDS: infiltration, measurement, prediction, modeling

Nomenclature

$\langle \ldots \rangle$	Indicates a time average of the quantity in arrows
C	Generalized shielding coefficient (see Table 1)
C_i	Pressure coefficient for a face
C_o	Internal pressure coefficient
C_p	Heat capacity of air, 1024 W/kg K
H	Height, m
H_s	Stack height of building (highest-lowest leak), m
H_t	Height of weather tower (wind measurement), m
H_w	Wind height of building (ceiling height above grade), m
L	Effective leakage area, m^2

[1]Staff scientist, Lawrence Berkeley Laboratory, Berkeley, CA 94720.

L_o Total leakage area of envelope, m^2
P Absolute pressure, Pa
Q Airflow (infiltration, ventilation), m^3/s
Q_{50} Airflow at 50 Pa, m^3/s
Q_{bal} Infiltration from balanced mechanical ventilation, m^3/s
Q_s Stack-induced infiltration, m^3/s
Q_{unbal} Infiltration from unbalanced mechanical ventilation, m^3/s
Q_w Wind-induced infiltration, m^3/s
$Q_{weather}$ Natural infiltration, m^3/s
R Fraction of total leakage area in the floor and ceiling
T Absolute (inside) temperature, 295 K
X Difference in ceiling/floor fractional leakage area
α Terrain coefficient (see Table 2)
β Dimensionless height (normalized by stack height of building)
β_o Position of the neutral level
f_s Stack factor
f_w Wind factor
g The acceleration of gravity, 9.8 m/s^2
γ Terrain exponent (see Table 2)
n Leakage exponent
q Specific infiltration (ratio of infiltration to leakage area), m/s
q_s Specific stack-induced infiltration, m/s
q_w Specific wind-induced infiltration, m/s
ρ The density of (outside) air, 1.2 kg/m^3
v Measured wind speed, m/s
v_* Free stream wind speed, m/s
v_1 Local wind speed, m/s
ΔP Outside-inside pressure difference, Pa
ΔP_o Leakage reference pressure, Pa
ΔT Inside-outside temperature difference, K

Because infiltration is a primary source of energy loss in residences, understanding the infiltration process is critical to any residential conservation program. Yet we are far more capable of calculating losses due to conduction than losses due to infiltration. Several explanations for this disparity can be stated. First, conduction losses are calculated more easily because the heat transfer is proportional to the temperature difference and does not depend strongly on any other driving force. Infiltration, on the other hand, depends on the interior-exterior point pressure difference but is not simply proportional to it. Furthermore, the driving pressure is caused by uncorrelated physical effects (wind speed and temperature difference). Second, conduction losses can be characterized by means of one parameter, thermal resistance, whereas infiltration, until now, has had no equivalent quantity.

The Lawrence Berkeley Laboratory (LBL) infiltration model was first pre-

sented in 1979 [*1*], and since that time we have been conducting an extensive refinement and validation program that includes both short-term and long-term data from a variety of sources. Our Mobile Infiltration Test Unit (MITU) has spent two successive winters making detailed measurements of weather, surface pressures, and infiltration. In this paper we will use data gathered from MITU and other sources to compare measurements with LBL model predictions.

Theory

The modeling of infiltration involves modeling many different effects. The behavior of air flowing through a leak in the building envelope under known pressures is determined from the fluid dynamics of pipe flow. These pressures, in turn, are a consequence of the interaction of the building and surrounding terrain with the weather. These considerations and others have been examined in great detail in a previous work [*2*] and will be summarized in the sections to follow.

Leakage Model

Leakage is the fundamental interaction of the envelope with the external pressures. As discussed in Ref *2*, the hydrodynamics of air flowing through cracks is quite complex; it involves laminar, transition, and turbulent flow through both rough and smooth paths. Rather than burden our infiltration model with a detailed synthesis of all crack parameters, we have chosen to make the assumption that the flow through a crack can be treated simply. The two simple physical choices are laminar and turbulent flow. As has been demonstrated with a measurement technique called AC pressurization [*3*], turbulent flow is the better assumption. This leads to an expression for the flow through a crack in terms of the square root of the pressure drop across it.

$$Q = L\sqrt{\frac{2\Delta P}{\rho}} \tag{1}$$

Thus, the quantity that characterizes the leakage has the units of area; we call it the effective leakage area. Leakage area can be thought of as the total amount of open area of a particular leakage site.

Superposition

Although we have a simple expression for the flow through the envelope as a function of pressure, it is not a simple matter to calculate the point pressures on the surface of a building. For weather-driven infiltration, there are two independent driving forces: wind and temperature difference (stack ef-

fect). Since, for the most part, the stack and wind effects are uncorrelated, we calculate their effect on infiltration independently; but, because both effects affect the internal pressure, we cannot simply add them to find the total infiltration. A detailed calculation of the total infiltration requires that the pressures be summed at each point and the flow calculated from that summation. We can, however, use our simplified leakage expression to combine the two independent parts; if the flow is proportional to the square root of the pressure, then two flows acting independently must add in quadrature.

$$Q_{\text{weather}} = \sqrt{Q_w^2 + Q_s^2} \tag{2}$$

This same superposition law can be used to combine other flows with the weather-induced flows. Specifically, if there is an exhaust fan operating, it will affect the internal pressure and thus be combined in quadrature. But, if there is a balanced ventilation system (for example, a counter-flow heat exchanger), the internal pressure will not be affected, and the balanced flow will simply add to the rest of the infiltration. Thus, our superposition expression combining both mechanical and naturally induced ventilation is as follows

$$Q = Q_{\text{bal}} + \sqrt{Q_{\text{unbal}}^2 + Q_w^2 + Q_s^2} \tag{3}$$

The terms Q_{bal} and Q_{unbal} can be calculated from the known supply and exhaust flows of the mechanical ventilation system.

$$Q_{\text{bal}} = \text{minimum of } (Q_{\text{supply}}, Q_{\text{exhaust}}) \tag{4.1}$$

$$Q_{\text{unbal}} = (Q_{\text{supply}} - Q_{\text{exhaust}}) \tag{4.2}$$

Thus, if there is exhaust but no supply, Q_{bal} will be zero and all the mechanical ventilation will be unbalanced.

Stack-Induced Infiltration

The stack effect is caused by the fact that the temperature at the body of air inside the building is different from the outside air temperature. This temperature difference causes a density difference and thus buoyancy, creating a pressure gradient along any vertical boundary. This pressure difference is a function of the temperature difference and the height above the neutral level.

$$\Delta P = \rho g H_s \frac{\Delta T}{T} (\beta_o - \beta) \tag{5}$$

The neutral level, β_o, is the (dimensionless) height at which the internal pressure and external pressure are equal; as we shall see, it is determined by the

requirement that air infiltration must equal air exfiltration. The stack height, H_s, is the height from the lowest leak in the envelope (normally the floor or ground level) and the highest leak in the envelope (normally ceiling level).

This expression gives the pressure at a particular height as a function of the temperatures involved. In a building, however, the leaks are distributed over the entire envelope, requiring a detailed summation. To avoid this level of detail, we have grouped the envelope leakage into three categories: floor, wall, and ceiling leakage area. Within each area we assume that the leakage is evenly distributed. Thus, we have three parameters that describe the leakage distribution: A_o, the total leakage area; R, the fraction of the leakage area in the floor and ceiling; and X, the difference in the fractional floor and ceiling leakage areas.

To calculate the stack infiltration, we must integrate the point pressures that are positive over the entire envelope

$$Q_s^+ = L_o \sqrt{\frac{gH_s}{2} \left| \frac{\Delta T}{T} \right| \beta_o} \left(R + X + \frac{4}{3} \beta_o \right) \tag{6.1}$$

and to calculate the exfiltration we must integrate all the negative point pressures

$$Q_s^- = L_o \sqrt{\frac{gH_s}{2} \left| \frac{\Delta T}{T} \right| (1 - \beta_o)} \left(R - X + \frac{4}{3} (1 - \beta_o) \right) \tag{6.2}$$

By continuity the infiltration and exfiltration must be equal. Equating these two quantities yields an expression for X in terms of β_o. Eliminating X from Eq 6 gives us one expression for the total stack effect infiltration.

$$Q_s = L_o \sqrt{2gH_s \left| \frac{\Delta T}{T} \right|} \frac{2}{3} (1 + R/2) \frac{\sqrt{\beta_o} \sqrt{1 - \beta_o}}{\sqrt{\beta_o} + \sqrt{1 - \beta_o}} \tag{7}$$

For convenience we define the stack factor as follows

$$f_s = \frac{2}{3} (1 + R/2) \frac{\sqrt{2\beta_o (1 - \beta_o)}}{\sqrt{\beta_o} + \sqrt{1 - \beta_o}} \tag{8}$$

In some instances it may be more desirable to use the ceiling-floor fractional leakage difference than the neutral level in the computation of the stack-induced infiltration. In this case we can use an approximate expression that relates the neutral level to the difference, and then the two equations become

$$Q_s = L_o \sqrt{gH_s \left| \frac{\Delta T}{T} \right|} \frac{(1 + R/2)}{3} \left(1 - \frac{X^2}{(2 - R)^2} \right)^{3/2} \tag{9}$$

$$f_s = \frac{(1 + R/2)}{3}\left(1 - \frac{X^2}{(2 - R)^2}\right)^{3/2} \tag{10}$$

Wind-Induced Infiltration

When wind impinges on or flows around a solid building, it induces a change in the pressure on the external faces of that building. This change in the surface pressure is proportional to the local wind speed and the shielding coefficient of that face.

$$\frac{dP_i}{dv} = C_i \beta v_1 \tag{11}$$

The pressure coefficient C_i is a function of wind angle and building orientation, and the resulting pressure must be summed over the entire exposed surface. Furthermore, there will be an internal pressure coefficient, C_o, which, like the neutral level for the stack effect, will be determined by requirement of continuity.

From numerical calculations using wind-tunnel data,[2] we have found that the wind-induced infiltration can be described by the following expression

$$Q_w = L_o v_1 C(1 - R)^{1/3} \tag{12}$$

The R dependency stems from the fact that the floor and ceiling are usually much more heavily shielded from the wind than are the walls. The generalized shielding coefficient, C, has been numerically calculated for 5° of obstruction around the building; the values are summarized in Table 1. Boundary layer wind tunnel data for an isolated structure [*4*] were used to calculate the coefficient for Shielding Class I; subsequent shielding classes were then approximated.

TABLE 1—*Generalized shielding coefficients.*

Shielding Class	C'	Description
I	0.324	no obstructions or local shielding whatsoever
II	0.285	light local shielding with few obstructions
III	0.240	moderate local shielding, some obstructions within two house heights
IV	0.185	heavy shielding, obstructions around most of perimeter
V	0.102	very heavy shielding, large obstruction surrounding perimeter within two house heights

[2]See Ref *2* for details of this numerical procedure.

Although the just-cited expression involves the use of the local wind speed at ceiling height, v_1, most wind data are taken from a weather tower not necessarily in the immediate vicinity. We, therefore, must convert the measured wind speed from a weather station into a local wind speed for our model. One of the standard methods for achieving this is: to convert the wind speed at the weather tower into the invariant velocity that is assumed to exist at the top of the atmospheric boundary layer, some 600 m above the surface; to move to the desired location; and to convert the invariant velocity into the local wind speed. The method we have chosen to use [5] yields essentially the same results but converts the wind speed to a free stream wind speed at 10 m instead

$$v = v_* \alpha \left(\frac{H}{10 \text{ m}} \right)^{\gamma} \tag{13}$$

The quantities α and γ are terrain-dependent parameters and are listed in Table 2. To convert the local wind speed into the weather tower wind speed, we must use the intermediate of the free stream wind speed.

$$v_1 = v \frac{\alpha_w \left(\frac{H_w}{10 \text{ m}} \right)^{\gamma_w}}{\alpha_t \left(\frac{H_t}{10 \text{ m}} \right)^{\gamma_t}} \tag{14}$$

Finally, then, we have an expression for the wind-induced infiltration.

$$Q_w = L_o v C (1 - R)^{1/3} \frac{\alpha_w \left(\frac{H_w}{10 \text{ m}} \right)^{\gamma_w}}{\alpha_t \left(\frac{H_t}{10 \text{ m}} \right)^{\gamma_t}} \tag{15}$$

TABLE 2—*Terrain parameters for standard terrain classes.*

Class	γ	α	Description
I	0.10	1.30	ocean or other body of water with at least 5 km of unrestricted expanse
II	0.15	1.00	flat terrain with some isolated obstacles
III	0.20	0.85	rural areas with low buildings, trees, or other scattered obstacles
IV	0.25	0.67	urban, industrial or forest areas or other built-up area
V	0.35	0.47	center of large city or other heavily built-up area

For convenience we define the wind factor as follows

$$f_w = C(1 - R)^{1/3} \frac{\alpha_w \left(\frac{H_w}{10\ \text{m}} \right)^{\gamma_w}}{\alpha_t \left(\frac{H_t}{10\ \text{m}} \right)^{\gamma_t}} \tag{16}$$

Wind direction has not been an explicit part of the model as described. But, if directional effects are judged to be important, they can be included by assigning a shielding class, and perhaps a terrain class, to each directional slice. An alternate measure would be to replace the constant shielding coefficient, C, with a smoothly varying function of angle (for example, $C = C_1 + C_2 \sin \theta$ could be useful for rowhousing). The choice of terrain and shielding classes is one made by inspection; these parameters are not to be treated as adjustable.

Vent-Induced Infiltration

The previous sections have dealt with the calculation of weather-induced infiltration through leaks and other pathways not principally designed for ventilation. In calculating the total ventilation, it is necessary to combine the airflows caused by the HVAC system with the naturally occurring ones. In a previous publication [*6*], we have shown how this can be done for a few simple mechanical systems; in general, it is necessary to calculate the airflow of the individual component (for example, exhaust vent, furnace flue, fireplace, etc.) and include its value in the total supply or exhaust flows. Superposition then can be used to find the total.

Summary of Model

We summarize the equations just derived.
Superposition

$$Q = Q_{\text{bal}} + \sqrt{Q_{\text{unbal}}^2 + Q_w^2 + Q_s^2} \tag{17}$$

Balanced (additional) ventilation

$$Q_{\text{bal}} = \text{minimum of } (Q_{\text{supply}}, Q_{\text{exhaust}}) \tag{18}$$

Unbalanced (additional) ventilation

$$Q_{\text{unbal}} = \text{maximum of } (Q_{\text{supply}}, Q_{\text{exhaust}}) - Q_{\text{bal}} \tag{19}$$

Stack-induced infiltration

$$Q_s = L_o f_s \sqrt{g H_s \left| \frac{\Delta T}{T} \right|} \tag{20}$$

Wind-induced infiltration

$$Q_w = L_o f_w v \tag{21}$$

Stack-factor

$$f_s = \frac{2}{3}(1 + R/2) \frac{\sqrt{2\beta_o(1 - \beta_o)}}{\sqrt{\beta_o} + \sqrt{1 - \beta_o}} \tag{22.1}$$

$$f_s = \frac{(1 + R/2)}{3} \left(1 - \frac{X^2}{(2 - R)^2}\right)^{3/2} \tag{22.2}$$

Wind factor

$$f_w = C(1 - R)^{1/3} \frac{\alpha_w \left(\frac{H_w}{10\text{ m}}\right)^{\gamma_w}}{\alpha_t \left(\frac{H_t}{10\text{ m}}\right)^{\gamma_t}} \tag{23}$$

Validation

An extensive validation effort was conducted over the course of several years to establish the limits and validity of our single zone model. Included in following paragraphs is a brief description of the validation effort and the results and conclusions thereof.

Short-term Measurements

The most commonly found type of infiltration data are in the form of short-term or spot measurements of leakage, weather, and infiltration. In these data sets, the infiltration usually was measured with a single tracer gas decay, the leakage with a blower door, and the weather with a portable tower. We have extracted from the literature [7–9] 15 different sites spanning the country from old conventional to new, energy-efficient designs and have compared our predicted infiltration to the measured infiltration.

The dashed lines in Fig. 1 represent the experimental error associated with the data; any points within them indicate that the model agrees to within experimental error. Taking the entire set of data, the predicted infiltration was on the average within 2% of the measured infiltration with a standard deviation of about 20%. This indicates that the predictions are quite good and can be expected to yield the correct results to within 20%. (The individual points for a particular house may be taken from different days. Therefore, the scatter of an individual set of measured infiltration values is not significant.)

Time-Series Data

One of the best tests of a physical model is not how well it can reproduce some average quantity from uncorrelated data, but rather how well it mirrors the physical situation and how well it can track changes in the physical quantities involved. In order to study the detailed behavior of infiltration, we built MITU [*10*], a full-scale test structure equipped with weather-, pressure-, and infiltration-measuring equipment. During the winters of 1981 and 1982, MITU was stationed in Reno, Nevada, and data were recorded.

Figure 2 compares the half-hour infiltration predictions with the measured infiltration as a function of time in MITU. Figure 3 shows data for MITU at the same location but during a more windy time.

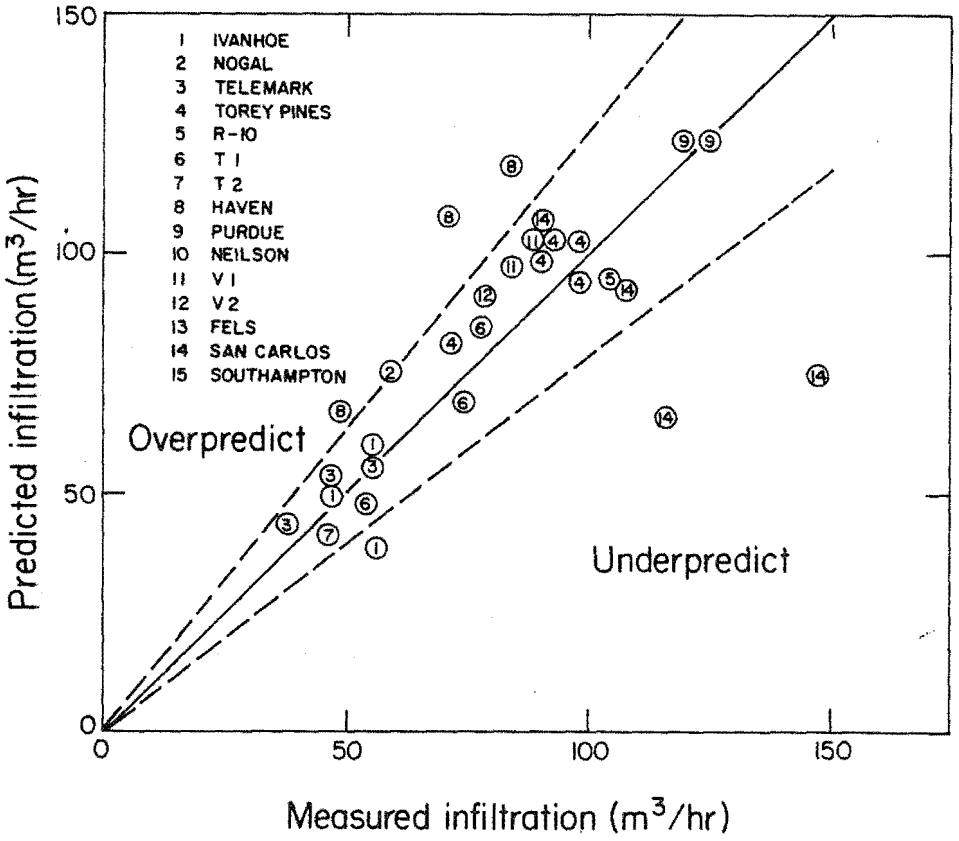

FIG. 1—*Short-term measurements below 150 m³/h.*

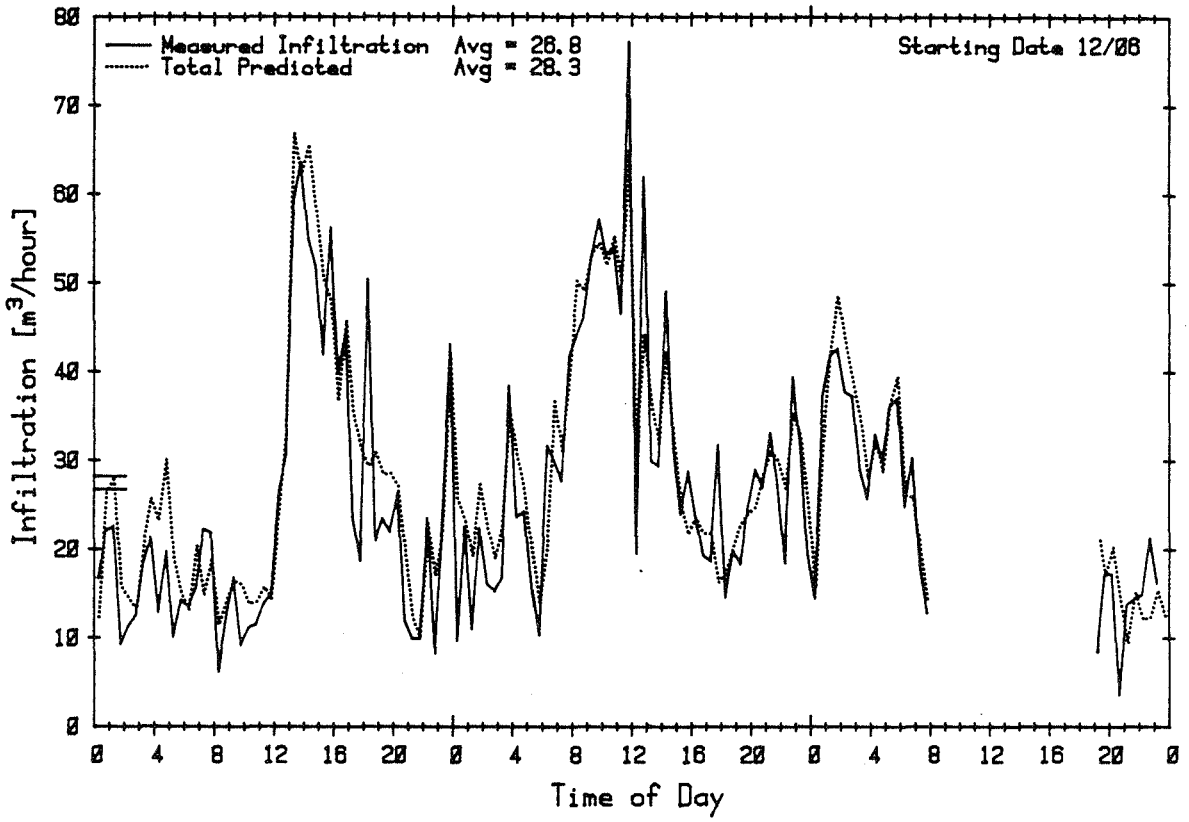

FIG. 2—*Predicted versus measured infiltration for a calm period.*

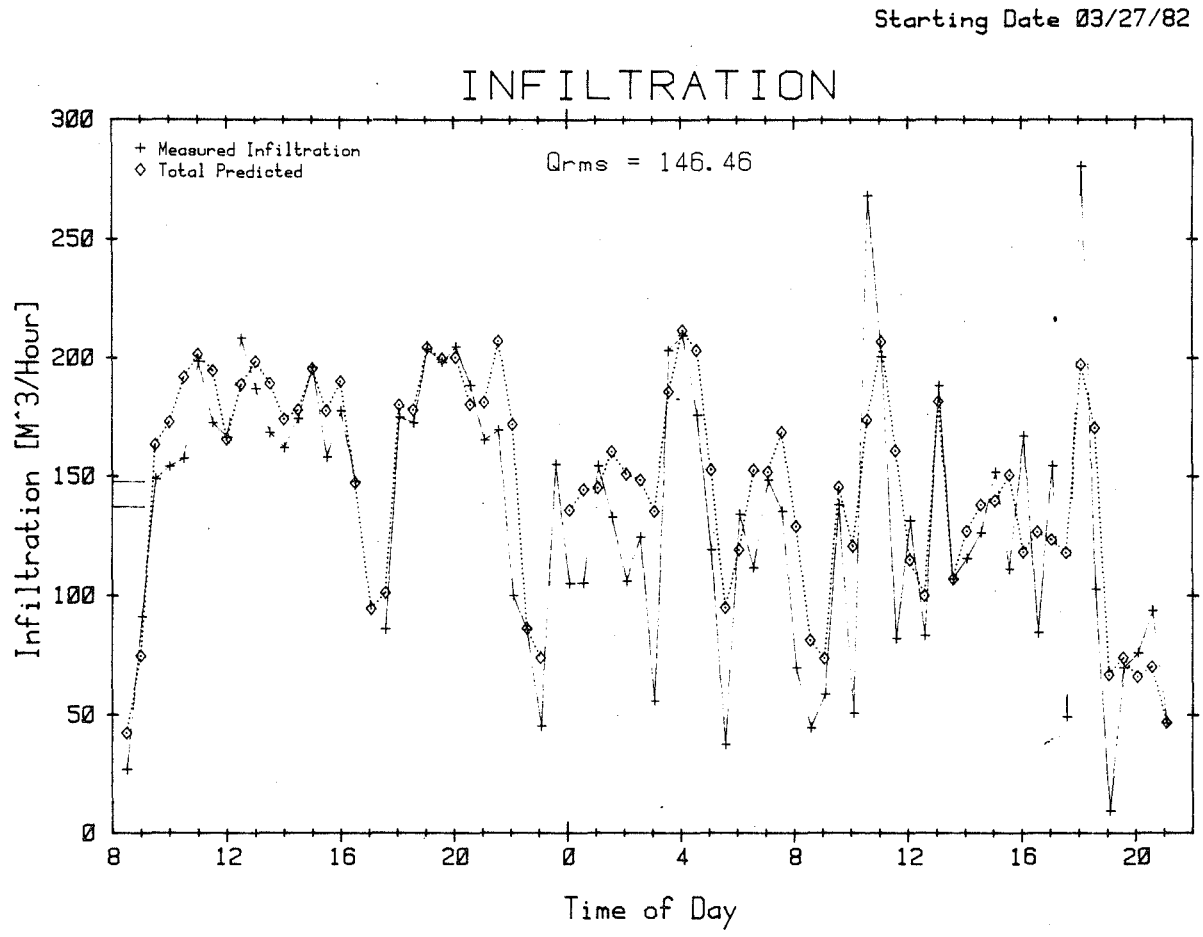

FIG. 3—*Predicted versus measured infiltration for a windy period.*

Both Figs. 2 and 3 show that the model has good tracking ability and can follow increases in infiltration caused by changes in the temperature and wind speed. Furthermore, the measured and predicted averages for the displayed data sets agree very closely; comparing these two figures indicates that the model behaves well over a wide range of infiltration rates.

Because MITU has a very simple, specially built structure, agreement of model predictions with MITU data is insufficient to validate the model. We, therefore, have used long-term data from other sources to help validate our model.

Figure 4 shows a set of data measured in an occupied test house in Rochester, New York [*11*]. This project was a joint effort with the New York State Energy Research and Development Authority and the Rochester Gas and Electric Company. Even though the predicted infiltration does not agree as well as it did with the MITU data, the model again tracks quite well and gives reasonable results considering the complications of occupancy.

We have used one additional set of long-term data [*12*] supplied to us by the Owens-Corning Fiberglas research center in Granville, Ohio. It consists of hourly data taken for 1 year on three (A, B, C) similar unoccupied houses.

Except in a very general way, the predicted and measured infiltration do not agree well. A close inspection of the data reveals a periodicity of the measured infiltration that does not match any periodicity of the weather patterns (Fig. 5). This periodicity, however, does match that of the system used to

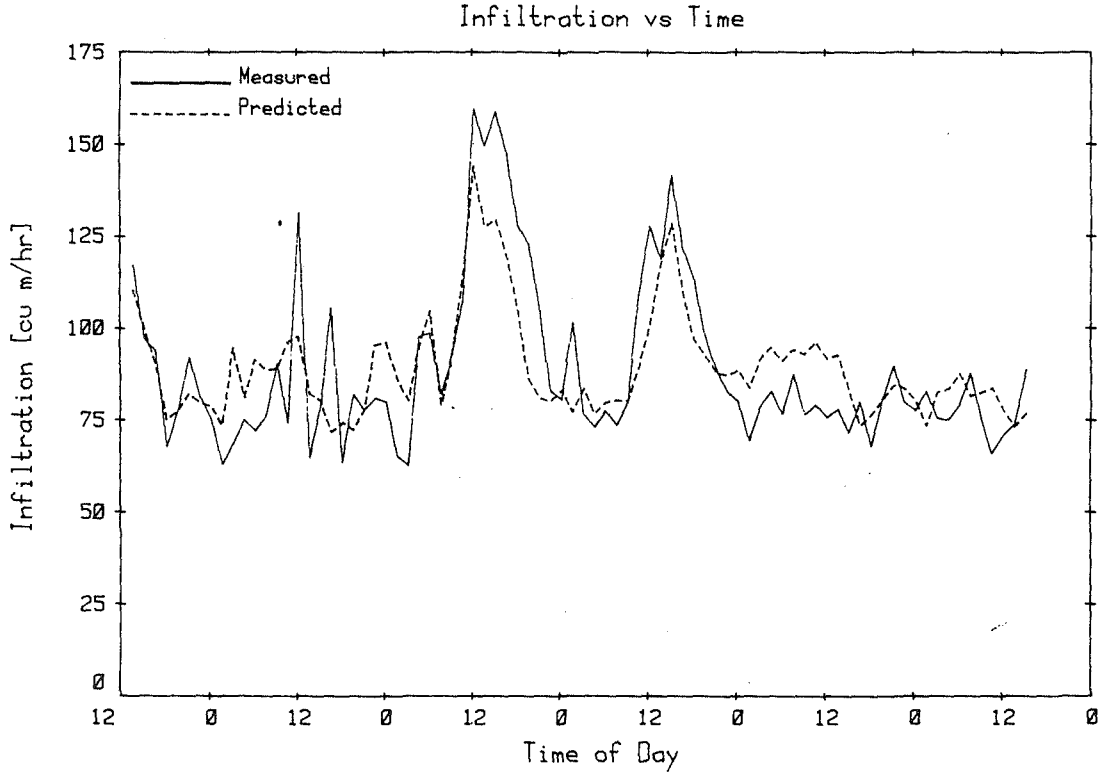

FIG. 4—*Predicted versus measured infiltration for Rochester house.*

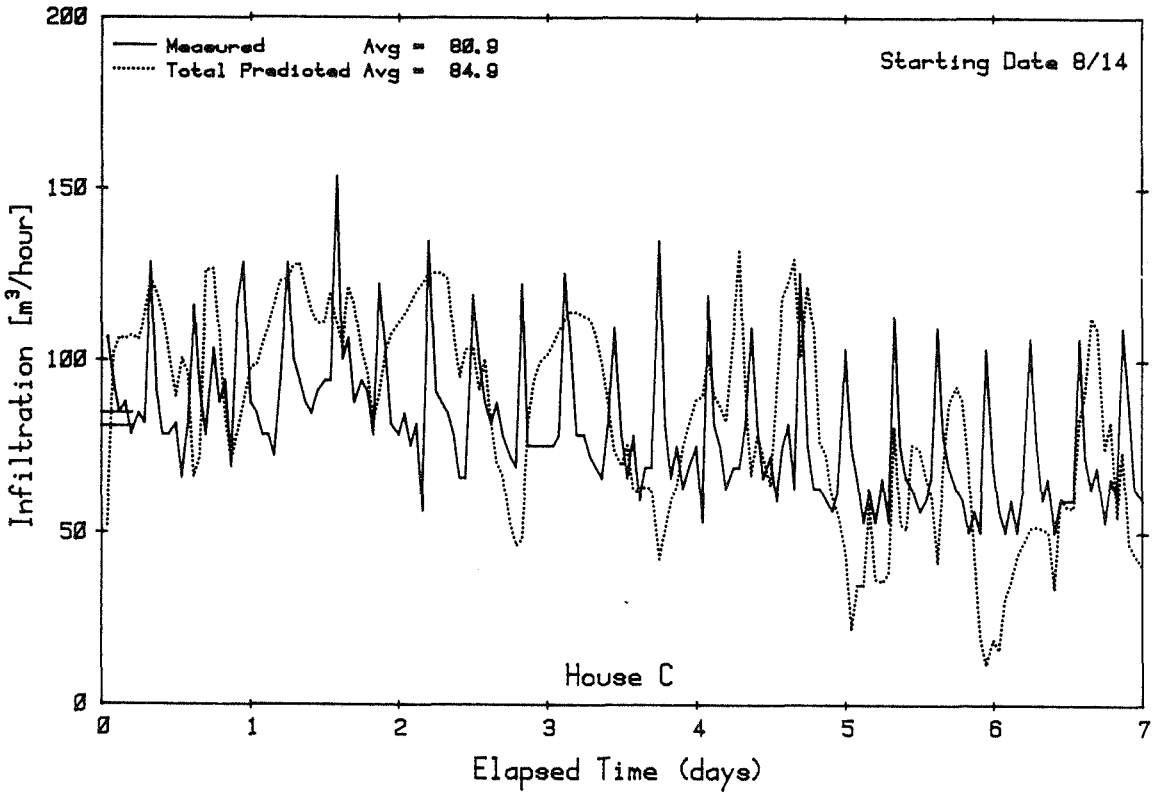

FIG. 5—*Infiltration for a one-week period in House C.*

inject and sample the tracer gas for the infiltration measurements. Unfortunately, this periodicity obscures the time-series behavior and, therefore, is unsuitable for tracking comparison.

Long-term Average

Although the tracking ability of a model is one of the most important validation aspects, the average behavior of the model over the long term can be as important. All the data points shown so far are individual points spaced no more than 1 h apart. In order to compare model behavior as we time average short-term infiltration variations, we group points together into rolling averages and compute the ratio of average predicted to average measured infiltration for different numbers of points. We then can make a histogram of the frequency of occurrence versus the ratio. In Figs. 6 through 9, we show histograms of the MITU data and the three Owens-Corning houses for unaveraged (that is, one point), one-day average, and one-week average data.

Figure 6(top) is a histogram of the half-hour measured points from MITU. The (geometric) mean of the ratio is 1.17, indicating that the mean of the distribution is 17% high. The spread factor of 1.34 indicates that there is a 34% spread around that mean. The shape of the distribution is recognizably Gaussian, indicating that the errors are reasonably random. As we move to longer term averages, the distribution becomes more peaked, indicating that

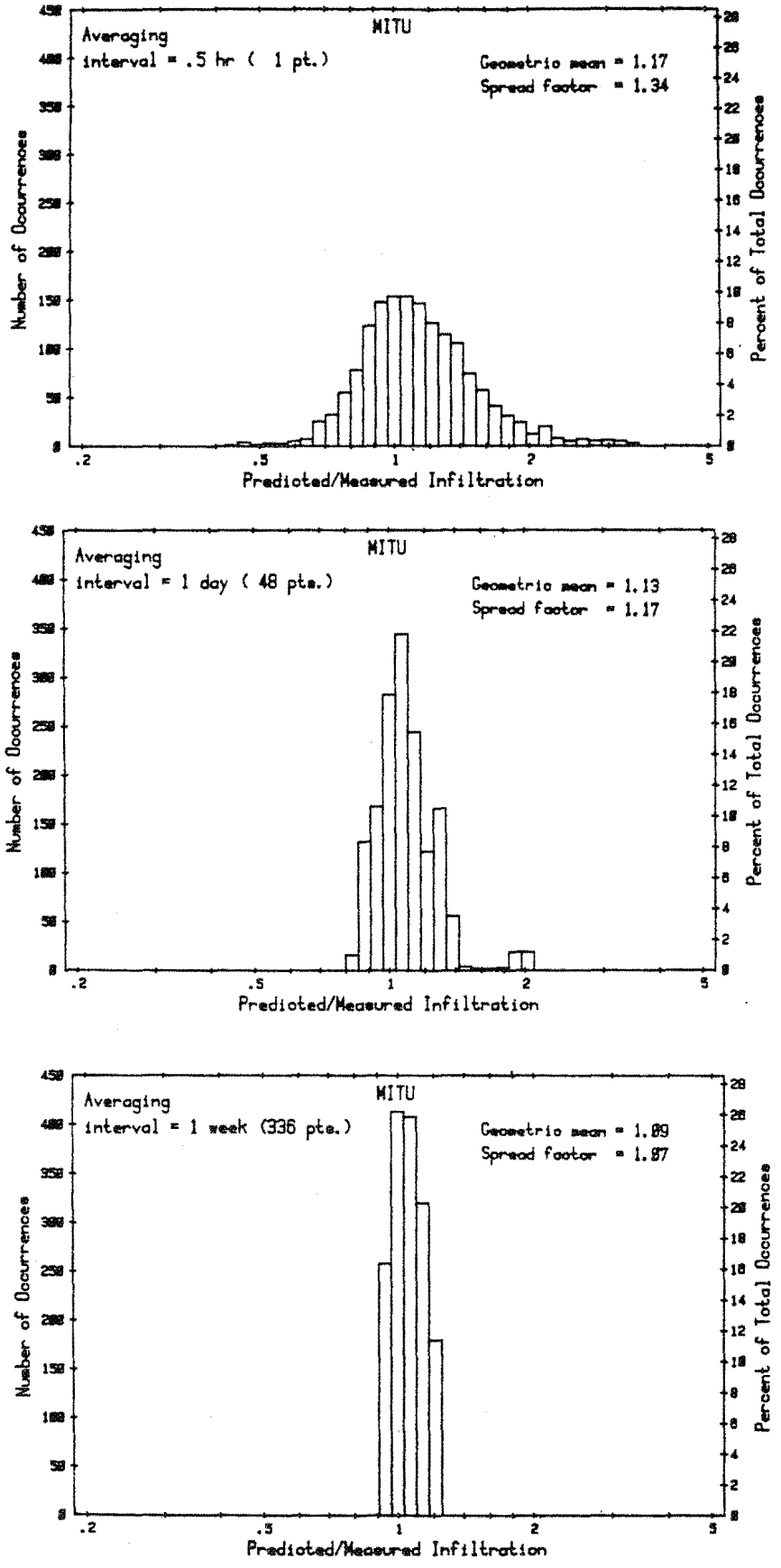

FIG. 6—*Histogram of MITU case.*

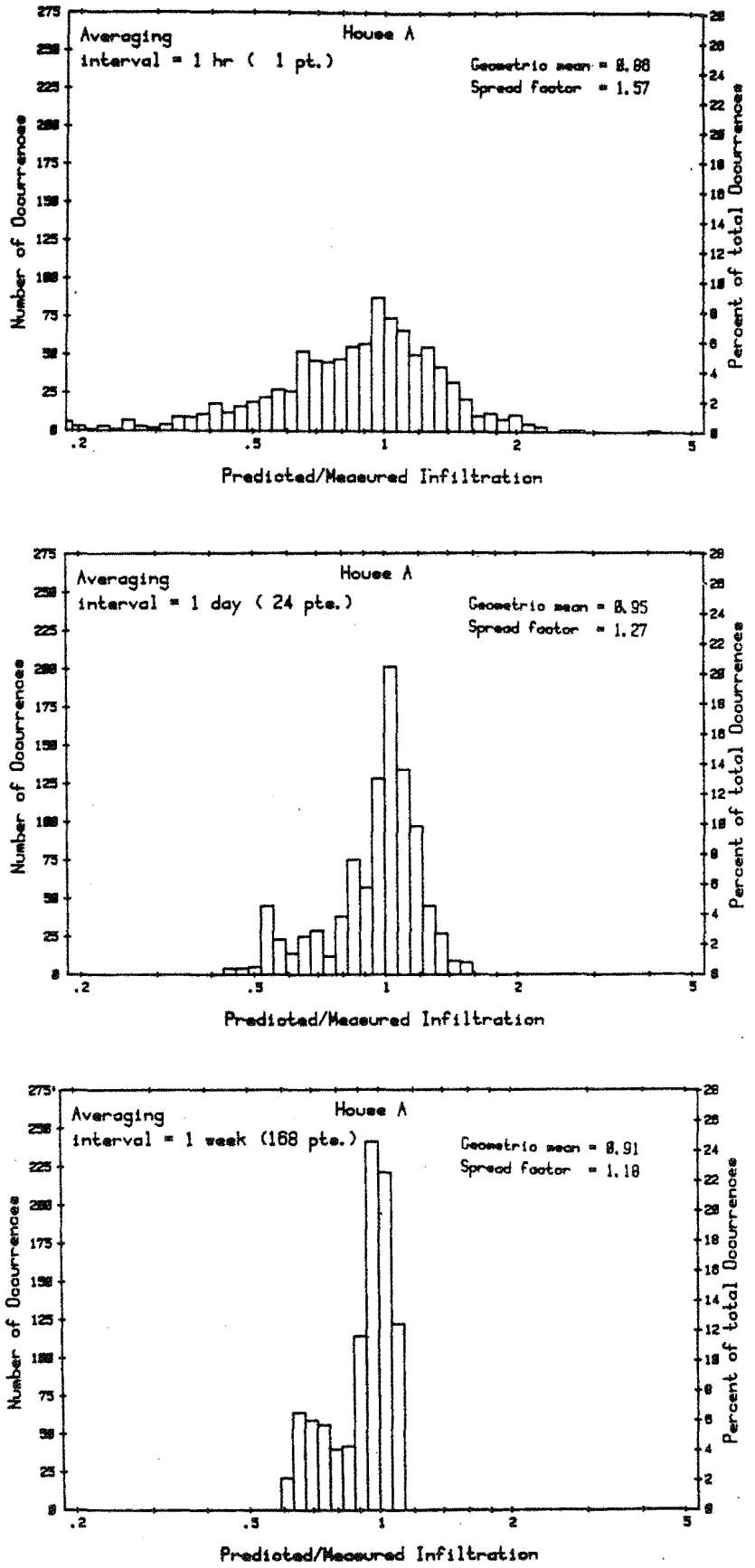

FIG. 7—*Histograms at three different averaging intervals for Owens-Corning Test House A.*

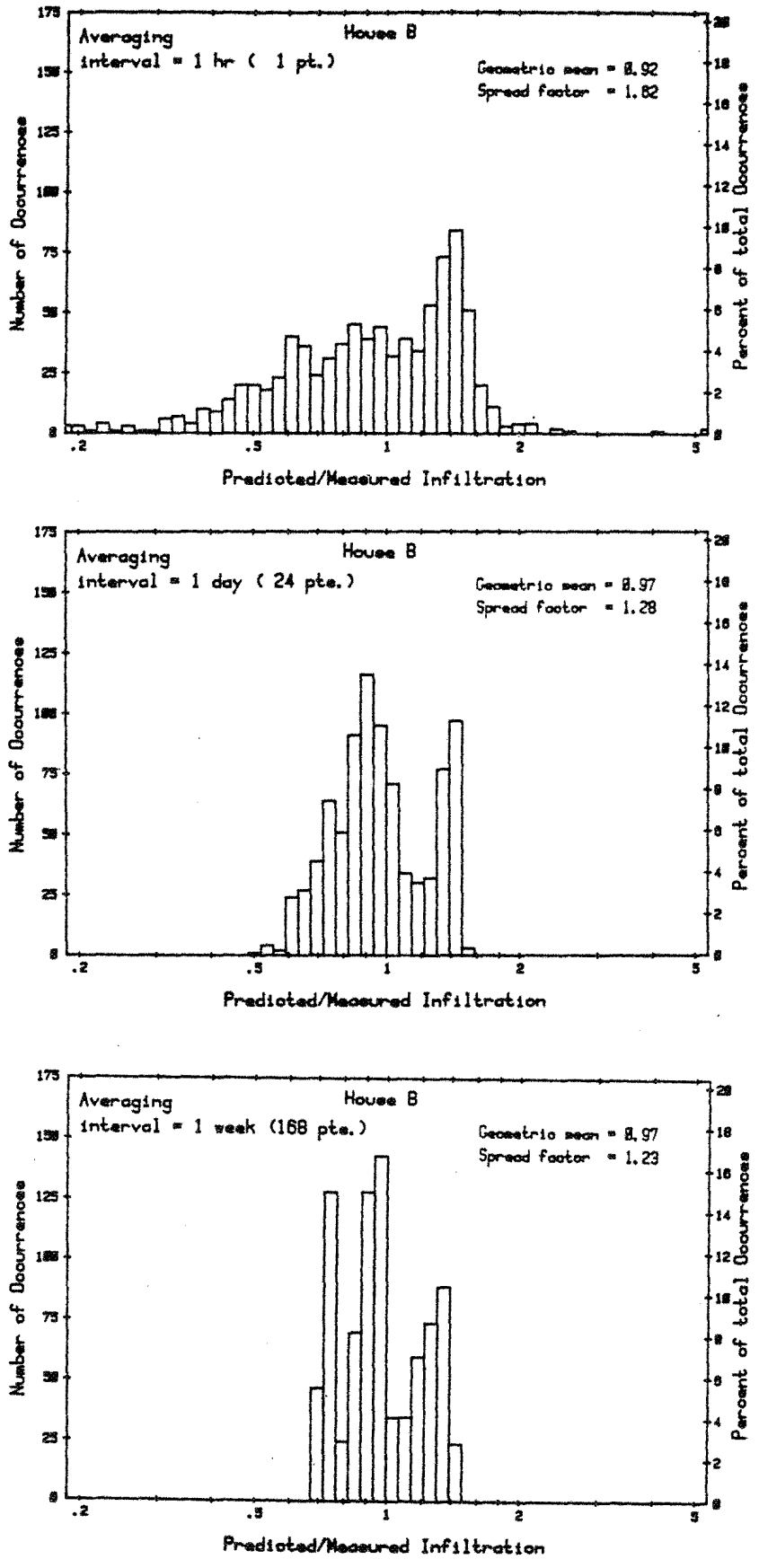

FIG. 8—*Histograms at three different averaging intervals for Owens-Corning Test House B.*

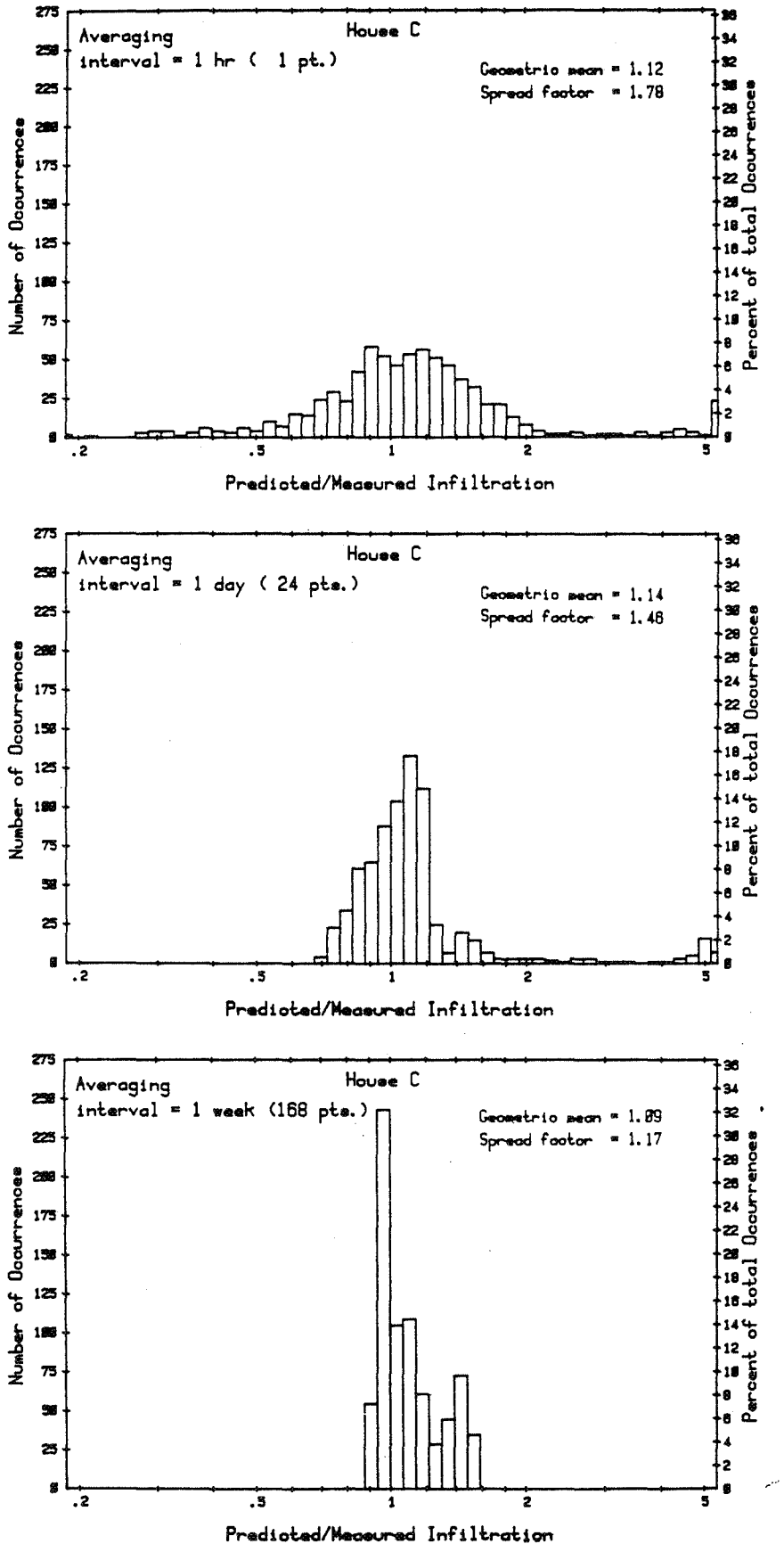

FIG. 9—*Histograms at three different averaging intervals for Owens-Corning Test House C.*

the spread of values is decreasing; furthermore, the mean value is approaching unity, suggesting perfect agreement. For one-week averages, the mean is only 9% high with a 7% spread around it. While it is expected that the distribution should become more peaked for longer averages, it is encouraging to see that the mean error gets smaller.

The next three figures (Figs. 7, 8, 9) are similar histograms for the three houses (A, B, C). In general, their behavior is the same; the spread decreases with longer averages. The mean values, however, are not as close to unity as they were for the MITU case, and (perhaps as a result of the periodicity) their shape is not as Gaussian.

If we take long-term average comparisons to their extreme, we get only one set of numbers to compare—those for the entire period of data taking. In Table 3 we compare the average measured infiltration, the average predicted infiltration, and the predicted average infiltration.

Note that for the MITU and Rochester data the three measures of infiltration agree to about 3%, but in the other three houses there is up to a 15% discrepancy.

The average measured and average predicted infiltration are the numerical averages of the individually measured data points. The predicted average infiltration is a single infiltration calculation made from average weather conditions (that is, average temperature difference and average wind speed). The accuracy of the predicted average infiltration is a measure of how good an estimate of infiltration will be when using only the average weather data for that period.

Detailed Examination

The previous sections have indicated the accuracy of the LBL model in an overall sense. We, however, can extract information about the strengths and weaknesses of the model by looking at a large set of data in great detail; only the MITU data set is both sufficiently large and well-defined. A detailed examination of this data set and comparison with a computer simulation already has been carried out [*13*], and some of the results will be presented herein.

TABLE 3—*Long-term average infiltration, m^3/h.*

Site	Average Measured	Average Predicted	Predicted Average
MITU	32.5	34.4	32.9
Rochester	89.7	89.4	82.9
House A	74.4	66.9	68.1
House B	72.9	75.7	80.3
House C	87.4	99.4	101.1

The entire MITU data sets from the winters of 1981 and 1982 have been used in this examination. The overall accuracy is given in Table 4.

The mean error is a measure of the bias of the model, that is, how far an average prediction will be from the true value (as given by the measured value). The standard deviation of the errors is a measure of the scatter of the model, or the range of error over which an individual prediction will vary. The smaller the bias, the better the long-term average prediction; thus, if only annual averages are desired, the only criterion for choosing a model would be its bias. The scatter, on the other hand, is a measure of how well the model follows short-term changes (that is, how well the model tracks).

The usefulness of this data set comes from the fact that it can be used to determine some of the sources of error (and, therefore, possible corrections) in the model.

Figure 10 bins all of the data by the measured infiltration value and then finds the mean error for each set of binned data. Any trend would indicate some systematic error in the model that scales with the actual infiltration. Since the infiltration is an indication of the total pressure across the leaks in the structure, any systematic error in the estimation of flow rate as a function of pressure could cause the observed trend. The fact that the trend in the error is downward with increasing infiltration implies that the model overpredicts at low pressures (that is, less than 4 Pa) and underpredicts at high pressures. This is traceable to the fact that the LBL model assumes an exponent of 0.5, and the measured exponent for MITU is 0.65.

Another source of error in a model can come from the calculation of infiltration in different regimes: specifically, stack- and wind-dominated flows. Figure 11 bins the data according to the ratio of stack-induced to wind-induced infiltration: a low value means wind-dominated flow and a high value implies stack-dominated flow. As in the previous figure, there are clear trends to the data. At very low values of the ratio, the model underpredicts; this is traceable to the choice of an average aspect ratio in the model, when, in fact, using the exact aspect ratio would improve the result. At stack/wind ratios

TABLE 4—*Measured infiltration versus LBL model predictions, m^3/h.*

Data Set	1981	1982	Total
Mean of measurements	40.4	45.4	42.7
Standard deviation of measurements	31.3 (77%)	40.9 (90%)	36.1 (85%)
Mean of predictions	45.1	49.1	46.8
Standard deviation of predictions	24.0	31.8	27.8
Mean of errors	4.7 (12%)	3.7 (8%)	4.1 (10%)
Standard deviation of errors	10.0 (25%)	13.5 (30%)	11.8 (28%)

NOTE—All percentages are relative to the mean measured infiltration.

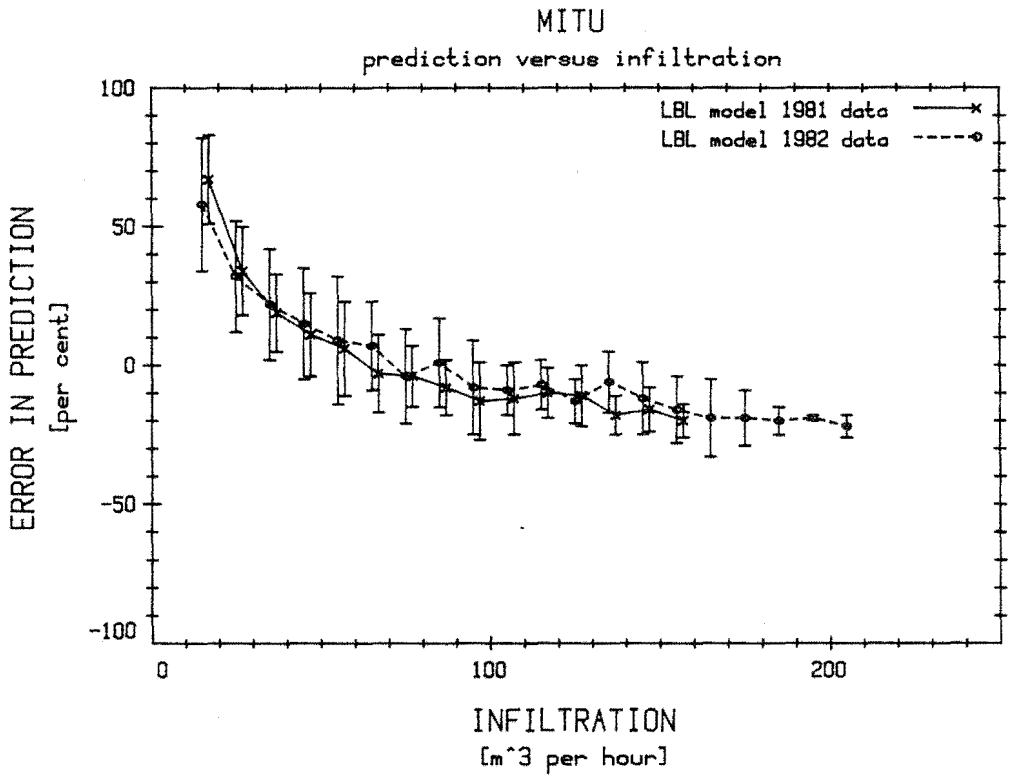

FIG. 10—*Errors in LBL model as a function of infiltration.*

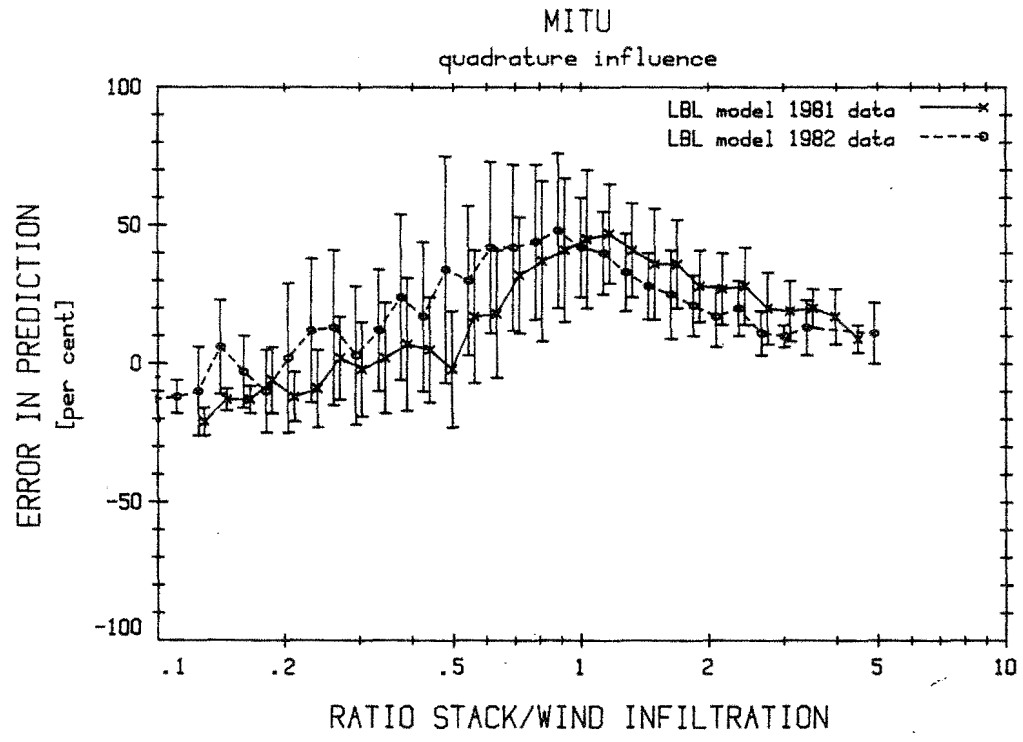

FIG. 11—*Errors in LBL model as a function of stack/wind ratio.*

near unity (that is, where the stack and wind effects are equivalent) the model overpredicts; this is traceable to the empirical method used to combine stack and wind effects (that is, quadrature addition), instead of a point-by-point addition of pressures (which would be impractical for a simplified model).

Wind direction can have a strong effect on the accuracy of any infiltration model. In the LBL model, wind direction is averaged, but the effects of that assumption can be seen by plotting the average error for different wind angle bins. In Fig. 12 we can see that for the simple rectangle of MITU the wind direction dependence is quite similar to the sinusoidal curve that one might estimate from first principles.

Future Work

In addition to defining the current accuracy of the infiltration model, the validation effort has indicated areas for future research. More work is necessary in the area of flow interactions; although each source of ventilation (that is, stack-induced, wind-induced, and mechanically induced supply and exhaust) may affect the pressure across the envelope differently, the LBL model combines them in a simple manner. The accuracy of this procedure should be investigated further, and modifications may be necessary to increase it. As shown in the detailed examination, other areas that could benefit from fur-

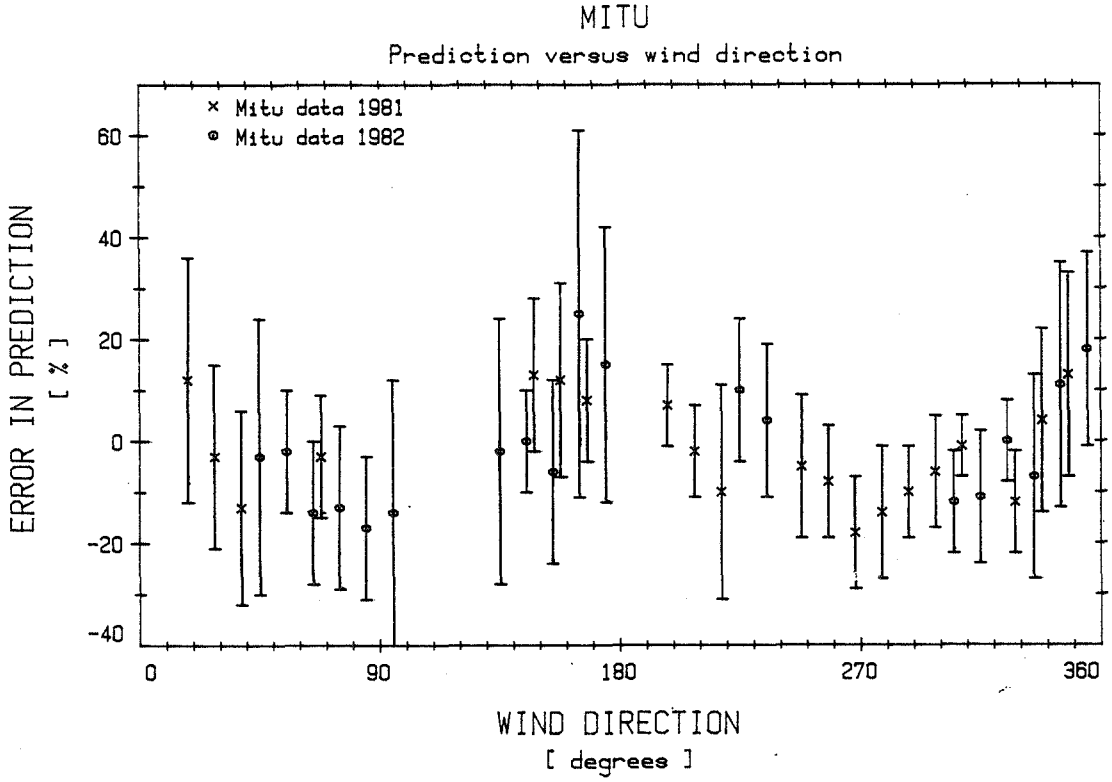

FIG. 12—*Errors in LBL model as a function of wind angle.*

ther study are directional dependence, wind-pressure coefficients, and flow-exponent calculations.

Summary

In this report we have presented the LBL infiltration model and have used field data to validate it. For short-term measurements, the model predicts to within 20% for well-defined environments (for example, the MITU trailer) and slightly higher for other situations. The long-term averages, however, tend to be more accurate. In MITU, the long-term (one week) average infiltration is accurate to 7%; in the Owens-Corning houses the long-term average error increases to up to 15%. A detailed examination of the LBL model using data from the MITU was used to probe the model and to suggest areas for future research.

Acknowledgment

This work was funded by the assistant secretary for Conservation and Community Systems, Buildings Division Office of Buildings and Community Systems, U.S. Department of Energy, under Contract No. DE-AC03-76SF00098.

References

[1] Sherman, M. H. and Grimsrud, D. T., *ASHRAE Transactions*, 86,II, 1980, pp. 778-807 (Lawrence Berkeley Laboratory Report, LBL-10163).

[2] Sherman, M. H., "Air Infiltration in Buildings," Ph.D thesis, University of California, 1980 (Lawrence Berkeley Laboratory Report, LBL-10712).

[3] Sherman, M. H., Grimsrud, D. T., and Sonderegger, R. C., "The Low Pressure Leakage Function of a Building," in *Proceedings of the DOE/ASHRAE Conference on the Thermal Performance Exterior Envelope of Buildings*, ASHRAE SP 28, American Society of Heating, Refrigerating and Air Conditioning Engineers, Atlanta, 1979 (Lawrence Berkeley Laboratory Report, LBL-9162).

[4] Akins, R. E., Peterka, J. A., and Cermak, J. E., in *Proceedings of the Fifth International Conference on Wind Engineering*, Pergamon Press, Elmsford, NY, 1980, pp. 369-380.

[5] "Recommendations for the Calculation of Wind Effects on Buildings and Structures," European Convention for Constructional Steelwork, Technical General Secretariat, Brussels, Belgium, Sept. 1978.

[6] Sherman, M. H. and Grimsrud, D. T., "A Comparison of Alternate Ventilation Strategies," in *Proceedings of the Third Air Infiltration Centre Conference*, London, United Kingdom, Sept. 1982 (Lawrence Berkeley Laboratory Report, LBL-13678).

[7] Grimsrud, D. T., Sherman, M. H., Blomsterberg, A. K., and Rosenfeld, A. H. in *Proceedings of the International Conference on Energy Use Management*, Vol. III, Pergamon Press, Elmsford, NY, 1979, pp. 1351-58, (Lawrence Berkeley Laboratory Report, LBL-9157).

[8] "Demonstration of Energy Conservation through Reduction of Air Infiltration in Electrically-Heated Houses," RP 1351-1, Johns-Mansville Research and Development Center, Denver, CO, 1979.

[9] Tamura, G. T., *ASHRAE Transactions*, 85,I, 1979, pp. 58-71.

[*10*] Blomsterberg, A. K., Modera, M. P., and Grimsrud, D. T., "The Mobile Infiltration Test Unit—Its Design and Capabilities: Preliminary Experimental Results," LBL-12259, Lawrence Berkeley Laboratory, Berkeley, CA, Jan. 1981.

[*11*] Sherman, M. H., Modera, M. P., and Grimsrud, D. T. in *Proceedings of the Third International CIB Symposium on Energy Conservation in the Built Environment*, Vol. VI, An Foras Forbartha, Dublin, 1982, pp. 6.A.1-10 (Lawrence Berkeley Laboratory Report, LBL-13520).

[*12*] Modera, M. P., Sherman, M. H., and Grimsrud, D. T., *ASHRAE Transactions*, 88,I, 1982, pp. 1351-72 (Lawrence Berkeley Laboratory Report, LBL-13509).

[*13*] Modera, M. P., Sherman, M. H., and Levin, P. A., "A Detailed Examination of the LBL Infiltration Model using the Mobile Infiltration Test Unit," *ASHRAE Transactions*, 89, 1983 (Lawrence Berkeley Laboratory Report, LBL-15636, 1983).